Molecular dynamics simulation of tool wear in elliptical vibration cutting: Case study on 3C-SiC

Changlin Liu[1], Jinyang Ke[2], Jianfeng Xu[2], Suet To[1, #]
[1] State Key Laboratory of Ultra-precision Machining Technology, Department of Industrial and Systems Engineering, The Hong Kong Polytechnic University, Hung Hom, Kowloon, Hong Kong
[2] State Key Laboratory of Intelligent Manufacturing Equipment and Technology, School of Mechanical Science & Engineering, Huazhong University of Science and Technology, Wuhan, China
Corresponding Author / Email: sandy.to@polyu.edu.hk, TEL: +852-2766-6587, FAX: +852-2362-5267

KEYWORDS: Molecular dynamics simulation, Elliptical vibration cutting, Silicon carbide, Tool wear

For the last few decades, elliptical vibration cutting (EVC) has been successfully applied in machining of many difficult-to-cut materials. During the machining process, the cutting tool usually vibrates in a high frequency and the transient material removal thickness ranges from a sub-nanometer level to a few nanometers. The interaction mechanism between cutting tool and workpiece is complicated and an in-deep understanding of the tool wear mechanism during EVC is required. In this research, molecular dynamics (MD) simulation was conducted to investigate the tool wear mechanism during EVC of monocrystalline 3C-SiC. Based on the proposed MD model, the tool vibration amplitude and nominal depth of cut in the simulation model is remarkably increased to describe the transient material removal feature in a single vibration cycle. The results indicates that during EVC, wear in the bottom of the tool edge mainly occurs in the initial stage of the vibration cycle while wear near the tool rake face can be observed in the extrusion-shear stage. According to the stress analysis, the tool rake face experiences obvious tensile stress in the extrusion-shear stage. The shape of the cutting tool is changed and compression of the material is observed with the propagation of crack, which can be identified as microchipping of the cutting tool. The results in this research could open a potential to improve the understanding in diamond tool wear mechanism during EVC.

1. Introduction

Silicon carbide (SiC), as one of the most important candidates of third-generation semiconductors with attracting physical/chemical properties [1]. However, the intrinsic hard brittle characteristics of 3C-SiC introduce great difficulties in ultra-precision cutting without obvious subsurface damage and cutting tool wear. For the last few decades, the ultrasonic vibration cutting technology has been successfully applied in machining of difficult-to-cut materials [2]. As the cutting tool is fed at a nominal cutting speed, the tool tip is controlled to vibrate elliptically in the plane determined by the nominal cutting direction and the chip flow direction. As fellows, the machining feasibility of many difficult-to-cut materials have been verified by applying the EVC technology.

When fabricating nanometric surface via EVC, the cutting tool usually vibrates in a high frequency and the transient material removal thickness ranges from a sub-nanometer level to a few nanometers. It has been revealed that EVC process demonstrates smaller Von Mises stress and less subsurface damage in workpiece than ordinary cutting [3]. Besides, thinning of the cutting chips can be observed during EVC process, which results an increase in the ratio of the uncut chip thickness to the cut chip thickness [4]. Furthermore, it has been verified that the vibration conditions in EVC including amplitude ratios, vibration frequencies, and phase differences have significant influences on the stress field in the workpiece [5], subsurface damage formation, and ductile-brittle transition [6]. For monocrystalline 3C-SiC, Zhao et al. [7] investigated the difference in the deformation mechanisms of monocrystalline 3C-SiC under EVC and ordinary cutting and discovered that cracking is significantly suppressed by applying EVC. Furthermore, They reported highly oriented high density stacking faults accompanied with suppressed amorphization and cracking in polycrystalline 3C-SiC in EVC, which contributes to significantly enhanced ductile material removal of the ceramic material compared to ordinary cutting [8].

In this paper, MD simulation is conducted based on the modified model [9] to investigate EVC of monocrystalline 3C-SiC. The material removal and tool wear mechanism in a single vibration cycle is studied. Large-scale Atomic/Molecular Massively Parallel Simulator (LAMMPS) [10] is applied to conduct the MD simulations, while the Open Visualization Tool (OVITO) [11] is employed to analyze the simulation results.

2. Molecular dynamics modelling

The MD model is presented in Fig. 1. To study the transient cutting mechanism in a single vibration cycle with acceptable computation cost, the workpiece is shaped according to the tool trajectory in the last vibration cycle [12]. As shown in Fig. 1c, T_b and T_o represent the bottom point and center point of the tool edge, respectively. For a blur tool, the surface generation point T_c continuously varies along the tool edge during cutting. The finished surface profile is generated by an envelope line of the tool edge, which is represented by the solid curve. Therefore, the trajectory of the transient surface generation point T_c can be calculated by:

$$x_c(t) = A_x \sin(2\pi f t) - vt - R\sin\theta(t) \tag{3}$$

$$z_c(t) = A_z \sin(2\pi f t + \varphi) + R(1 - \cos\theta(t)) \tag{4}$$

where $\sin\theta(t) = \dfrac{z'(t)}{\sqrt{x'(t)^2+z'(t)^2}}$ and $\cos\theta(t) = \dfrac{-x'(t)}{\sqrt{x'(t)^2+z'(t)^2}}$.

Following the classic MD cutting model, workpiece and cutting tool are divided into boundary region, thermostat region, and Newton region. Atoms in the boundary region are fixed in their balanced positions to hold the workpiece. Atoms in the thermostat region are kept at the ambient temperature to dissipate the generated cutting heat. While the atoms in the Newton region follow the Newton's second law of motion. The shape of boundary region and thermostat region follows the tool trajectory with translation in minus x and z direction to keep the enough distance between the cutting zone and the fixed boundaries. Both the fixed region and thermostat region have a thickness of 1 nm. The boundary conditions include a periodic boundary along the y axis and fixed boundaries in x and z axis, which are adopted to simulate the constraint of the adjacent materials on the cutting zone. The analytical bond order potential (ABOP) [13] is applied to describe the atomic interactions since it demonstrates an adequate approximation of mechanical properties of diamond structures [14].

The cutting tool was set as deformed body to investigate the tool wear behavior during the vibration cycle, as illustrated in Fig. 2. The tool edge radius is set as 5nm, and the tool arc radius was adopted as 6.5nm in this study. Furthermore, a chamfering of 3nm is induced to construct smooth surface on the diamond tool. It is worth noting that the cutting speed is found to have significant influence on the temperature in the cutting zone and thus could influence the critical undeformed chip thickness due to the thermal effect. In previous MD simulation of EVC, the cutting speed usually ranges from 50m/s to 200 m/s. Attributed to the modification on MD model, the cutting speed adopted in this study is set as 3m/s, which is much closer to experimental values. The nominal cutting orientation is $[\bar{1}00]$ direction on (001) plane. In addition, to investigate the influence of the tool trajectory and cutting temperature on the material removal feature, numerical experiments are conducted with various cutting temperature and vibration amplitude A_x. Details of the simulation parameters are listed in Table 1.

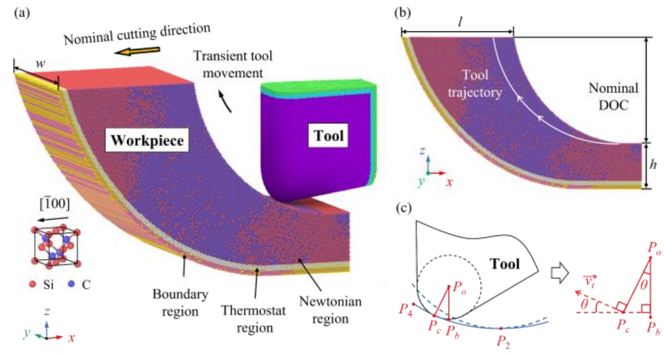

Fig. 1 Model of the EVC simulation: (a) illustration of the MD model. (b) (c): Determination of the workpiece morphology.

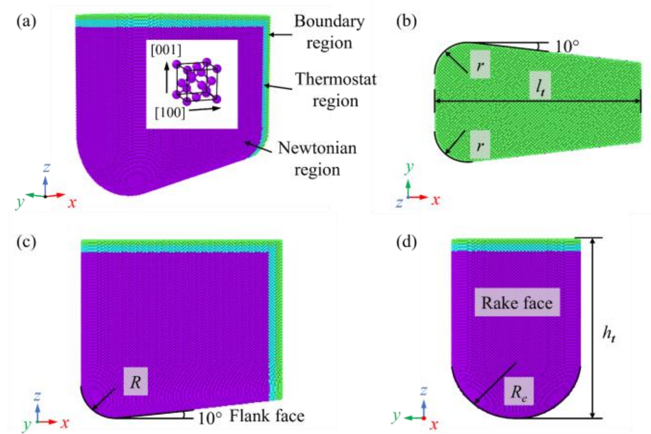

Fig. 2 Construction of the Diamond tool.

Table 1. Parameters of the MD simulation model.

Parameters	Value
$l \times h \times w$	30 × 10 × 24nm
Nominal Cutting direction	(001) / $[\bar{1}00]$
Tool rake/clearance angle	0°/10°
Ambient temperature	300K
Vibration frequency f	500MHz
Phase difference φ	90°
Vibration amplitude A_x / A_z	25-35/25nm
Nominal DOC	25nm
Tool edge radius R	3.57nm
Tool arc radius R_0	6.5nm
Nominal cutting speed	3m/s

3. Results and discussion

3.1 Cutting tool wear

Fig. 3 demonstrates the atomic configuration of the cutting tool wear observed in this simulation. The wear atom is simply defined as those atoms experience bond breaking and have lost their crystal structure. After cutting, a part of the wear atoms is detached from the cutting tool and left on the machined surface, while other wear atoms are adhered on the flanks face near the cutting tool edge. By tracing the position of the wear atoms before cutting, it can be concluded that the abrasion mainly occurs on the cutting tool edge near the flank face, which is similar to the observation in ordinary cutting [15].

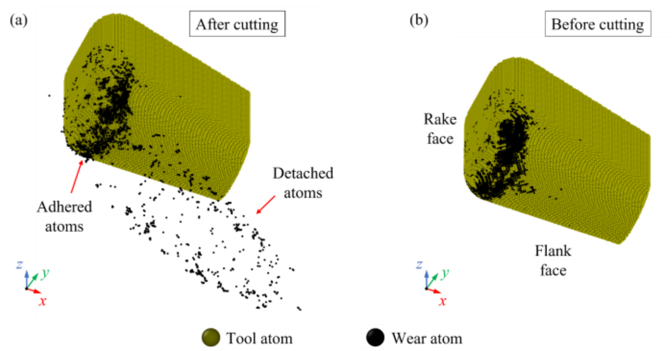

Fig. 3 Snapshot of the tool abrasive wear.

To demonstrate the relationship between wear behavior and material removal process, the wear atoms are colored based on the simulation timestep that the wear event occurred, as shown in Fig. 4a. It is observed that wear in the bottom of the tool edge mainly occurs in the initial stage of the vibration cycle, namely in the extrusion stage. As the cutting tool proceeds, some wear atoms near the tool rake face are observed. Fig. 4b counts the number of generated wear atoms as a function of the simulation timestep. It can be concluded that most wear atoms present in the extrusion and extrusion-shear stage. In addition, obvious deformation of the cutting tool causes internal stress in diamond, which is an important mechanism of tool wear and failure. The distribution of hydrostatic stress in the cutting tool under extrusion and extrusion-shear stage are given out in Fig.5. In the extrusion stage, the high compressive region concentrates in the cutting tool edge near the tool flank face. While in the extrusion-shear stage, the high compressive region moves along the tool edge and locates near the tool rake face. Furthermore, it is worth noticing that the tool rake face experiences obvious tensile stress in the extrusion-shear stage, which might cause crack and fracture of the cutting tool.

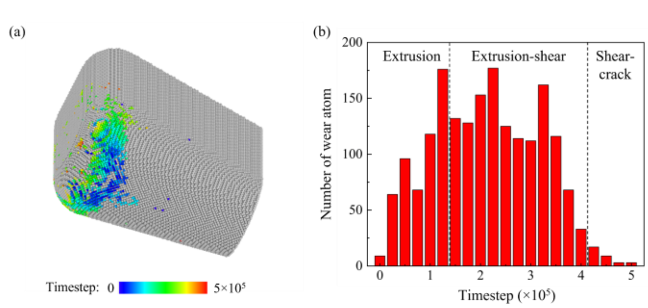

Fig. 4 (a) Color map of the wear atoms. (b) Number of generated wear atoms as a function of the simulation timestep.

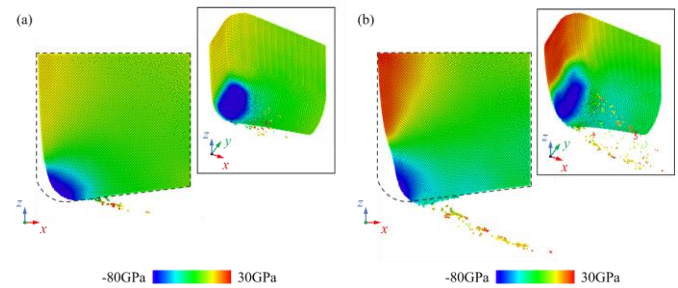

Fig. 5 Distribution of hydrostatic stress in the cutting tool at (a) extrusion and (b) extrusion-shear stage.

3.2 Effect of vibration amplitude on tool wear

Fig. 6 presents the number of wear atoms at the end of cutting when A_x was set as 25nm, 30nm, and 35nm. With the increase of A_x, the transient cutting speed and the contact distance between tool and workpiece is increased. Therefore, although the transient material removal thickness is decreased, the abrasion of cutting tool is promoted and more wear atoms are generated. Fig. 7a demonstrates the color map of the generation timestep for wear atoms. It is observed that more wear atoms are generated on the cutting tool edge near the tool flank face when A_x is increased. Furthermore, the distribution of generation frequency of wear atoms is present in Fig. 7b. Since the tool trajectory become less steep with the increase of A_x, the dominant material removal mechanism of extrusion is promoted and the extrusion to shear transition is delayed. Therefore, the peak of wear atom generation appears later with larger A_x. and more wear atoms are generated near tool flank face due to abrasion.

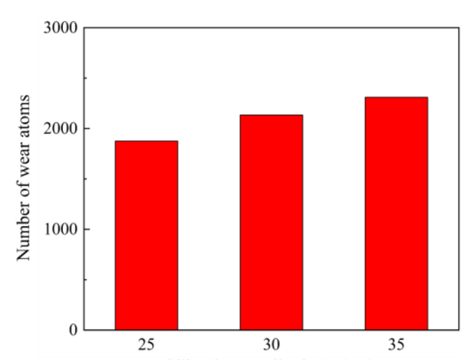

Fig. 7 Number of wear atoms with increased vibration amplitude A_x.

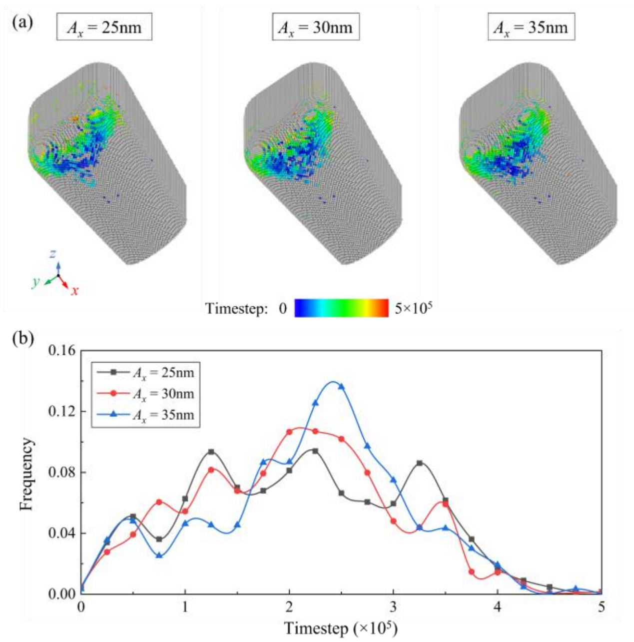

Fig. 8 Generation of the wear atoms at different A_x. (a) Color map of the generation for wear atoms. (b) Frequency of generated wear atoms as a function of the simulation timestep.

4. Conclusion

In this paper, the classic MD model is modified to investigate the material removal mechanism and tool wear in a single vibration cycle during elliptical vibration cutting (EVC) process. The dominant wear mechanism can be different in a single- vibration cycle. It can be concluded that most wear atoms present in the extrusion and extrusion-shear stage. In addition, obvious deformation of the cutting tool causes internal stress in diamond, which is an important mechanism of tool wear and failure.

ACKNOWLEDGEMENT

This work was funded by the Research Grants Council of the Hong Kong Special Administrative Region, China (Project No.: PolyU 15221322),

REFERENCES

1. Q. Li, J. F. Wang, F.-F. Yan, J.-Y. Zhou, H.-F. Wang, H. Liu, L.-P. Guo, X. Zhou, A. Gali, Z.-H. Liu, Z.-Q. Wang, K. Sun, G.-P. Guo, J.-S. Tang, H. Li, L.-X. You, J.-S. Xu, C.-F. Li, G.-C. Guo, Room-temperature coherent manipulation of single-spin qubits in silicon carbide with a high readout contrast, National Science Review 9 (2022) nwab122.
2. E. Shamoto, T. Moriwaki, Study on Elliptical Vibration Cutting, CIRP Annals 43 (1994) 35-38.
3. B. Zhu, D. Zhao, H. Zhao, J. Guan, P. Hou, S. Wang, L. Qian, A study on the surface quality and brittle–ductile transition during the elliptical vibration-assisted nanocutting process on monocrystalline silicon via molecular dynamic simulations, RSC Advances 7(2017) 4179-4189.
4. S. Goel, F.D. Martinez, S.Z. Chavoshi, N. Khatri, C. Giusca, Molecular dynamics simulation of the elliptical vibration-assisted machining of pure iron, Journal of Micromanufacturing 1 (2018) 6-19.
5. H. Dai, H. Du, J. Chen, G. Chen, Influence of elliptical vibration on the behavior of silicon during nanocutting, The International Journal of Advanced Manufacturing Technology (2019).
6. C. Liu, J. Zhang, J. Zhang, X. Chen, J. Xiao, J. Xu, A simulation investigation on elliptical vibration cutting of single-crystal silicon, The International Journal of Advanced Manufacturing Technology 108 (2020) 2231-2243.
7. L. Zhao, J. Zhang, J. Zhang, A. Hartmaier, Atomistic investigation of machinability of monocrystalline 3C–SiC in elliptical vibration-assisted diamond cutting, Ceramics International 47 (2021) 2358-2366.
8. L. Zhao, J. Zhang, J. Zhang, A. Hartmaier, T. Sun, Formation of high density stacking faults in polycrystalline 3C-SiC by vibration-assisted diamond cutting, Journal of the European Ceramic Society 42 (2022) 5448–5457.
9. C. Liu, J. Zhang, J. Zhang, J. Chu, X. Chen, J. Xiao, J. Xu, Numerical investigation on material removal mechanism in elliptical vibration cutting of single-crystal silicon, Materials Science in Semiconductor Processing 134 (2021) 106019.
10. S. Plimpton, Fast parallel algorithms for short-range molecular dynamics, Journal of Computational Physics 117 (1995) 1-19.
11. A. Stukowski, Visualization and analysis of atomistic simulation data with OVITO–the Open Visualization Tool, Modelling and Simulation in Materials Science and Engineering 18 (2010) 015012.
12. X. Zhang, A.S. Kumar, M. Rahman, K. Liu, Modeling of the effect of tool edge radius on surface generation in elliptical vibration cutting, The International Journal of Advanced Manufacturing Technology 65 (2012) 35-42.
13. P. Erhart, K. Albe, Analytical potential for atomistic simulations of silicon, carbon, and silicon carbide, Physical Review B 71 (2005) 035211.
14. S. Goel, X. Luo, R.L. Reuben, H. Pen, Influence of temperature and crystal orientation on tool wear during single point diamond turning of silicon, Wear 284-285 (2012) 65-72.
15. J. Yan, Z. Zhang, T. Kuriyagawa, Mechanism for material removal in diamond turning of reaction-bonded silicon carbide, International Journal of Machine Tools and Manufacture 49 (2009) 366-374.